

Cite this: *RSC Adv.*, 2016, 6, 5774

Characterization of regio- and stereo-selective sulfation of bufadienolides: exploring the mechanism and providing insight into the structure–sulfation relationship by experimentation and molecular docking analysis†

Jing Ning,^{‡a} Yonglei Cui,^{‡a} Chao Wang,^{‡ac} Peipei Dong,^a Guangbo Ge,^b Xiangge Tian,^a Jie Hou,^a Xiaokui Huo,^a Baojing Zhang,^a Tonghui Ma^d and Xiaochi Ma^{*ac}

Bufadienolides are a major class of bioactive compounds derived from amphibian skin secretion. Recent studies demonstrate that bufadienolides have a promising role in targeted cancer chemotherapy. However, extensive metabolism and inactivation strongly restrict the clinical applications of bufadienolides. This study aimed to systematically characterize the sulfation of six representative bufadienolides (including bufalin, resibufogenin, cinobufagin, bufotalin, telocinobufagin and deacetylcinobufagin) in amphibian skin secretion and to provide insight into the structure–sulfation relationship by experimentation and molecular docking analysis with series of bufadienolides and derivatives. For all the six representative bufadienolides, one corresponding monosulfate was detected in the incubation mixtures. The sulfates were accurately identified as bufadienolides 3-*O*-sulfates by NMR and HPLC-MSⁿ techniques. Reaction phenotyping studies using human recombinant sulfotransferase (SULT) and liver S9 demonstrated that SULT2A1 mediated the formation of bufadienolide 3-*O*-sulfate with a high specific selectivity. Further kinetic evaluation demonstrated that deacetylcinobufagin could be used as a preferred probe of SULT2A1. The regio- and stereo-selective sulfation properties of SULT2A1 and the structural variation effects of bufadienolides were investigated by docking analysis, which revealed the significance of appropriate molecule orientation and hydrophobic interactions of motifs with SULT2A1 His99 residues. Additionally, significant differences between humans and animal species were observed in the sulfation of bufalin and resibufogenin. This study provided important data for elucidating the mechanisms of bufadienolide sulfation and leads to a better understanding of the bufadienolide–SULT interaction which can be further used in preclinical development and rational use of bufadienolides.

Received 22nd October 2015
Accepted 4th January 2016

DOI: 10.1039/c5ra22153f

www.rsc.org/advances

Introduction

Bufadienolides, characterized by the presence of a six-membered lactone (α -pyrone) ring located at position C17 β ,

are a class of cardiac steroids rich in amphibian skin secretion.^{1,2} They have a profound effect in increasing the contractile force of the heart by inhibiting the enzyme Na⁺, K⁺-ATPase and are widely prescribed for patients with cardiovascular disease in Asia.³ For the last few years, bufadienolides have manifested significant potential applications in cancer therapies and may represent a promising form of targeted cancer chemotherapy.⁴ It was recently evidenced that bufadienolides (including bufalin, resibufogenin, cinobufagin and its analogues) are the primary constituents responsible for the antitumor activity of huachansu (cinobufacini injection) which is an intravenously administered extract of toad venom which has been used for cancer treatment for hundreds of years.^{5–7} Bufadienolides have attracted the attention of scientists worldwide, leading to in-depth investigations of their bioactivity and pharmacological actions. These compounds have been found to be involved in

^aCollege of Pharmacy, Academy of Integrative Medicine, Dalian Medical University, Dalian, China. E-mail: maxc1978@163.com; Fax: +86-411-86110419; Tel: +86-411-86110419

^bLaboratory of Pharmaceutical Resource Discovery, Dalian Institute of Chemical Physics, Chinese Academy of Sciences, Dalian, China

^cState Key Laboratory of Bioactive Substance and Function of Natural Medicines, Institute of Materia Medica, Chinese Academy of Medical Sciences and Peking Union Medical College, Beijing, China

^dCollege of Basic Medical Science, Dalian Medical University, Dalian, China

† Electronic supplementary information (ESI) available. See DOI: 10.1039/c5ra22153f

‡ These authors contributed equally to this work.

complex cell-signal transduction pathways and have the ability to regulate cell growth, differentiation, apoptosis and glucose metabolism in human tumors.^{8–10} Currently, the increasing demands for the discovery and development of natural products for cancer therapy have challenged scientists to expedite the process for the drug ability assessment of bufadienolides.

However, collective evidences suggest that bufadienolides are subjected to extensive metabolism in human and animals.^{11–14} The metabolism and pharmacokinetics study indicated that bufadienolides were well-absorbed and rapidly eliminated from systemic circulation,^{11–14} that the half-life is only 6 minutes in rat after intravenous administration of resibufogenin.¹⁴ Our previous studies have demonstrated that CYP3A4 mediated hydroxylation is involved in the metabolism of series of bufadienolides in human.^{3,15,16} However, our latest study found that bufadienolides were significantly sulfated in human primary hepatocytes, which indicated that sulfation was an important route in their metabolism. Since the sulfates of bufadienolides exhibited much less potency than the parent agent,^{17,18} the sulfation could be considered a clearance and inactivation pathway of bufadienolides which play an important role in the modulation of their exposure level and bioactive effects.

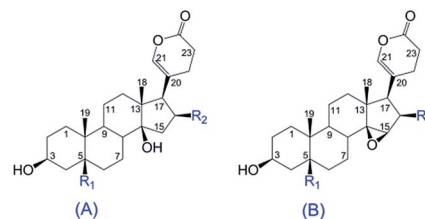
Understanding of sulfotransferases (SULT) substrate specificity is of great importance in predicting contribution of sulfation to substrate and metabolite disposition *in vivo*. Among the identified human SULT enzymes, the major isoforms expressed in adult liver are SULT1A1, SULT1A3, SULT1B1, SULT1E1, and SULT2A1.^{19,20} Investigation on the interaction between steroids and SULT demonstrated that SULT2A1 and SULT1E1 are common SULT responsible for the sulfation of steroids,²⁰ while other isoform sometimes is involved in the sulfation reaction. Bufadienolides possess typical steroid nucleus, while α -pyrone substituent at C17 is an evidently characteristic that distinguish from other steroids. It implied that the SULT bufadienolides specificity may different from the knowledge has been acquired and provide the ground for the optimization of bufadienolides. However, there is thus far no investigation to uncover the structural bases for the sulfation selectivity and structural variation on the catalytic efficacy of bufadienolides by SULT.

In this study, the objectives were to systematically characterize of the sulfation of six representative bufadienolides in amphibian skin secretion and to elucidate the structure–sulfation relationship by using series of bufadienolides and its derivatives. This study will provide important data for elucidating the mechanisms and effects of sulfation on bufadienolides metabolism and lead to a better understanding of the bufadienolide–SULT interaction which can be further used in medicinal chemistry to optimize the chemical structures of bufadienolides. And these findings also may offer guidance for the rational use and the preclinical development of bufadienolides.

Results

Sulfation of the bufadienolides by human primary hepatocyte and human liver S9

One metabolite was detected when the six bufadienolides, including BF, RB, CB, BFT, TCB and DCB (Fig. 1), were



Bufadienolides	Basic structure	R1	R2
Bufalin (BF)	A	H	H
Telocinobufagin (TCB)	A	OH	H
Bufofalin (BFT)	A	H	OAc
Resibufogenin (RB)	B	H	H
Cinobufagin (CB)	B	H	OAc
Deacetylcinobufagin (DCB)	B	H	OH

Fig. 1 Chemical structures of the main bufadienolides in amphibian skin secretion.

incubated with human liver S9 (HLS9) in the presence of 3'-phosphoadenosine-5'-phosphosulfate (PAPS). The products of the different bufadienolides were detectable and identified as important metabolites in human hepatocytes. For all bufadienolides, the m/z values for the $[M - H]^-$ of the metabolite in human hepatic S9 increased 80 when compared with the corresponding parent compounds (Fig. S1†). This indicated that the metabolites were monosulfate conjugates of bufadienolides.

Identification of the sulfate conjugates of bufadienolides

To determine the metabolic site of RB, the sulfate metabolites of different bufadienolides were synthesized *in vitro* and further identified by ^1H and ^{13}C -NMR spectra. The carbon signals were assigned and are listed in Table S1.† For example, compared with RB, a significant upfield shift ($\Delta\delta + 9.4$) was observed at the C3 position, this was assigned a sulfuric acid at the C3 position. Therefore, the sulfate metabolite of RB was identified as an RB-3-sulfate. Similarly, the metabolites of other bufadienolide were also identified as 3-*O*-sulfates.

Assays by recombinant human SULT isoforms

The six representative bufadienolides were incubated with the recombinant human SULT (rhSULT), including 1A1*1, 1A1*2, 1A2, 1A3, 1B1, 1E1 and 2A1, to identify the SULT isoforms responsible for the conjugation reaction. At three substrate concentrations, the sulfate conjugates were exclusively formed by SULT2A1; no other metabolite was observed under the same incubation conditions (Fig. 2). The sulfation rate of RB at the 1 μM substrate concentration was 2.60 nmol per min per mg SULT2A1, which was higher than the other bufadienolides. Among the six major bufadienolides, the sulfation rates of BF, RB, CB and BFT significantly decreased following increases in substrate concentrations.

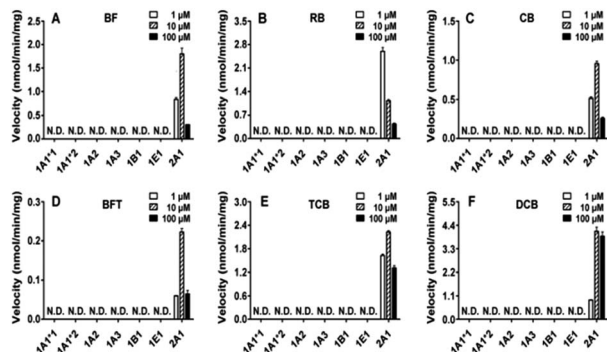


Fig. 2 Sulfation of the six bufadienolides by human recombinant SULTs.

Chemical inhibition study

Seven selective inhibitors/substrates of major SULT isoforms were used to screen the SULTs responsible for the formation of bufadienolides sulfates in HLS9. Dehydroepiandrosterone (DHEA), which is a selective substrate for SULT2A1, significantly inhibited the sulfation reaction of bufadienolides (Fig. 3) to less than 10% activities. In contrast, the selective inhibitors/substrates of other SULT isoform showed negligible inhibitory effects (less than 20% inhibition, $p < 0.05$). To further determine the primary role of SULT2A1 in the sulfation of the six bufadienolides, we determined the inhibitory effects of DHEA with different concentrations. The results showed that DHEA exhibited a similar inhibitory profile toward SULT2A1 and HLS9-mediated sulfations of the examined bufadienolides (Fig. S2 and Table S2[†]). The collectively results strongly suggest

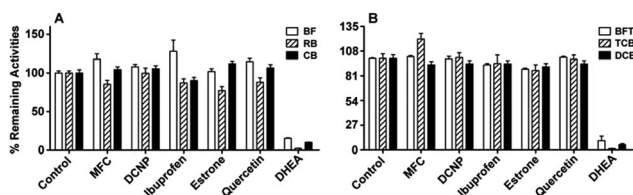


Fig. 3 Effects of selective SULT inhibitors/substrate on the formation of bufadienolides sulfates in human liver S9.

that SULT2A1 was primarily responsible for the sulfation of these bufadienolides in the human liver.

Additionally, it was evident that the sulfations of BF and RB were catalyzed predominantly by SULT2A1 in liver S9 from various animal species (Fig. S3[†]). These findings suggested the potential similarity in the metabolic enzymes for RB and BF sulfations in liver S9 from different animal species.

Kinetics characterization

The kinetics analyses of the six representative bufadienolides in amphibian skin secretion were performed in HLS9, recombinant SULT2A1 and the combined recombinant SULT (Fig. 4). The substrate inhibition model was fitted to the kinetics profile for the 3-O-sulfation of bufadienolides in HLS9 and SULT2A1. The kinetics parameters of the sulfation of the six bufadienolides were determined and are listed in Table 1.

When the kinetics parameters among the six bufadienolides obtained in HLS9 and SULT2A1 and the combined recombinant SULTs were compared, the K_m and V_m were varied extensively. In HLS9, it was found that RB showed the lowest K_m (0.35 μM) and the highest intrinsic clearance (628.6 μL per min per mg protein), which was dozens-fold lower and hundreds-fold higher than those of BFT (7.77 μM and 3.6 μL per min per mg protein, respectively). The K_m and V_{max} values of TCB in HLS9 were slightly varied with those of RB; thereafter, the TCB exhibited a relatively large intrinsic clearance among the six bufadienolides. Additionally, SULT2A1 exhibited a medium affinity and catalytic capacity toward CB, BF and DCB. The affinity and intrinsic clearances were similar among all bufadienolides obtained with SULT2A1, HLS9 and the combined recombinant SULTs. This implied that SULT2A1 was primarily responsible for catalysing the sulfation of bufadienolides in human liver.

For other bufadienolide derivatives, our results showed that the bufadienolides with 3- α -OH were not effectively catalyzed by rhSULT2A1. The sulfate metabolite of OCB was undetectable under the same incubation conditions as those treated with the six representative bufadienolides. Additionally, the apparent K_m of rhSULT2A1-mediated sulfation was determined (Fig. S4 and Table S3[†]). Although there were small differences in the

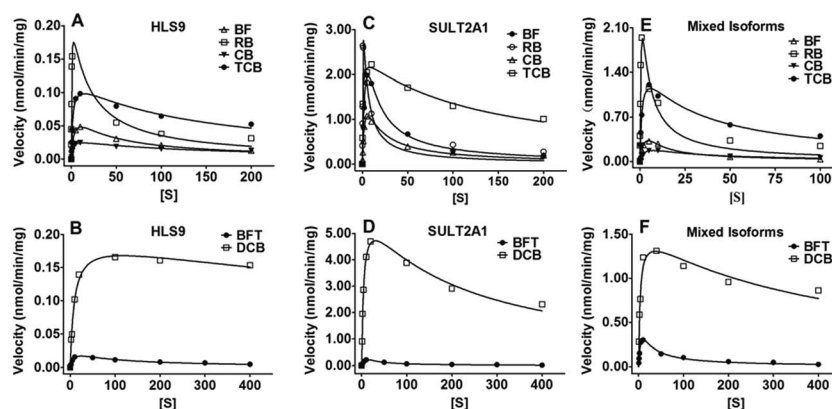


Fig. 4 Kinetic plots of the six representative bufadienolides sulfation in HLS9 (A and B), rhSULT2A1 (C and D) and mixed isoforms (E and F).

Table 1 Kinetic parameters of the six representative bufadienolides sulfation in HLS9, human recombinant SULT2A1, and the combined human recombinant SULT

Compounds	Enzymes	V_m (nmol per min per mg)	K_m (μ M)	K_{si} (μ M)	V_m/K_m (μ L per min per mg)
BF	HLS9	0.0763 ± 0.0056	3.19 ± 0.50	36.9 ± 5.1	23.8
	SULT2A1	6.15 ± 1.03	6.63 ± 1.49	5.86 ± 1.38	927.6
	Mixed isoforms	1.20 ± 0.42	6.18 ± 2.72	3.42 ± 1.61	194.2
RB	HLS9	0.221 ± 0.023	0.353 ± 0.071	19.0 ± 3.6	628.6
	SULT2A1	4.87 ± 0.95	0.451 ± 0.163	3.15 ± 1.11	10 822.2
	Mixed isoforms	3.85 ± 0.81	0.676 ± 0.242	2.73 ± 0.92	5746.3
CB	HLS9	0.030 ± 0.002	1.45 ± 0.21	119.5 ± 18.4	20.7
	SULT2A1	2.11 ± 0.27	2.95 ± 0.62	12.2 ± 2.8	715.3
	Mixed isoforms	0.297 ± 0.032	2.57 ± 0.48	20.8 ± 4.2	112.8
BFT	HLS9	0.028 ± 0.003	7.77 ± 1.72	79.2 ± 17.0	3.6
	SULT2A1	0.982 ± 0.454	21.9 ± 12.5	8.00 ± 4.31	44.6
	Mixed isoforms	0.705 ± 0.102	6.58 ± 1.40	15.5 ± 3.1	106.4
TCB	HLS9	0.123 ± 0.011	1.69 ± 0.24	125.4 ± 17.9	71.0
	SULT2A1	2.42 ± 0.10	0.482 ± 0.086	128.2 ± 20.0	5041.7
	Mixed isoforms	1.60 ± 0.11	1.15 ± 0.18	29.0 ± 5.1	1391.3
DCB	HLS9	0.193 ± 0.015	8.97 ± 1.35	1526.0 ± 607.3	21.2
	SULT2A1	6.12 ± 0.31	4.50 ± 0.58	205.0 ± 26.92	1360.0
	Mixed isoforms	1.55 ± 0.12	3.53 ± 0.78	397.6 ± 113.2	439.1

structures of the bufadienolides, the K_m varied up to a thousand-fold. CBFT exhibited the lowest K_m (0.29 μ M) and BFE exhibited the largest K_m (228 μ M). Grouped by the K_m values, CBFT, RB and TCB displayed markedly high affinities for SULT2A1; however, BFT, AB, GB, PBFE and BFE exhibited low affinities for SULT2A1.

Correlation studies

The sulfation rates for DHEA and various bufadienolides were determined using S9 from individual human liver ($n = 16$). Correlation analyses were conducted for the sulfations of DHEA and bufadienolides. It found that the sulfation velocities of BF, RB, CB, BFT, TCB and DCB were significantly correlated with DHEA sulfation velocities (Fig. S5†) with correlation coefficients (r) of 0.954, 0.919, 0.941, 0.937, 0.973 and 0.956, respectively. This evidence indicated that SULT2A1 played a dominant role in the sulfation of bufadienolides in human livers.

Interspecies difference in bufadienolide sulfation

It is well-accepted that the choice of a suitable animal model with similar metabolic mechanisms as humans is crucial for results in drug trials because there are species-dependent species-specific effects and toxicities.²² Comparing *in vivo* pharmacological and pharmacokinetic in the present study, the interspecies differences in the sulfations of RB and BF (*i.e.*, the compounds with the highest catalytic capacities and biological activities) were studied using liver S9 obtain from monkey (CyLS9), mini-pig (PLS9), dog (DLS9), rabbit (RaLS9), guinea pig (GLS9), rat (RLS9) and mouse (MLS9).

The sulfate conjugates of the bufadienolides were analyzed after RB and BF were incubated with liver S9 from different animals (except for DLS9 and MLS9). Kinetic studies were then performed to compare the abilities to catalyze the sulfation of RB and BF (Fig. 5 and Table 2). Among the animal liver S9

studied, RLS9 exhibited the lowest affinity for BF and RB, and the K_m values were approximately 7-fold and 10-fold larger than those of HLS9, respectively. It was observed that the catalytic activity of RaLS9 was higher than those of HLS9 and liver S9 from other mammals, which resulted in a relatively large hepatic *in vitro* intrinsic clearance (V_m/K_m) for the 3-*O*-sulfate of BF and RB.

Molecular docking studies

Molecular docking was carried out to explore the interaction model between bufadienolide derivatives and SULT2A1. All the bufadienolide derivatives (Fig. 1 and S4†) could dock into the active pocket of SULT2A1. Assuming these analogues were capable of binding with the enzyme in similar conformations, we selected a reasonable bioactive mode from the top five

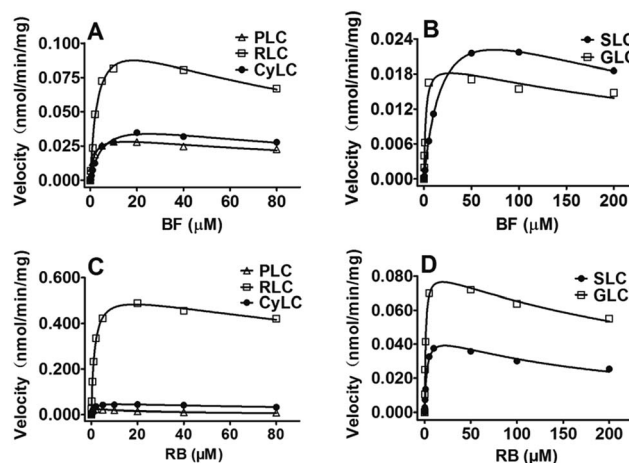


Fig. 5 The Kinetic plots of BF (A and B) and RB (C and D) sulfation in liver S9 from monkey, mini-pig, rabbit, guinea pig and rat.

Table 2 Kinetic parameters of BF and RB sulfation in liver S9 from monkey (CyLS9), mini-pig (PLS9), rabbit (RaLS9), guinea pig (GLS9) and rat (RLS9)

Compounds	Enzymes	V_m (pmol per min per mg)	K_m (μ M)	K_{si} (μ M)	V_m/K_m (μ L per min per mg)
BF	CyLS9	48.1 ± 4.2	5.38 ± 0.89	119.1 ± 30.31	8.9
	PLS9	33.7 ± 1.1	2.18 ± 0.28	127.8 ± 25.63	16.5
	RaLS9	116.6 ± 7.9	3.02 ± 0.58	118.6 ± 32.42	66.2
	GLS9	20.6 ± 1.8	2.04 ± 0.40	250.6 ± 79.95	10.8
	RLS9	34.9 ± 0.9	21.3 ± 1.0	256.5 ± 17.73	1.6
RB	CyLS9	52.7 ± 1.6	1.13 ± 0.09	127.1 ± 16.03	46.9
	PLS9	26.9 ± 0.9	0.242 ± 0.032	26.99 ± 2.78	112.5
	RaLS9	555.9 ± 13.6	1.41 ± 0.093	251.8 ± 39.0	390.1
	GLS9	85.4 ± 2.6	1.11 ± 0.11	368.3 ± 60.0	75.7
	RLS9	47.9 ± 2.1	2.32 ± 0.38	215.5 ± 40.3	20.3

conformations ranked by their Hammett scores. The substrates in the 3- β -OH group formed hydrogen bonds with His99 (Fig. 6A–L) which was the key site of SULT2A1 that interacting with the classical substrate DHEA.²¹ However, for OCB, EBF, ERB and EDCB, there were no hydrogen bonding interactions between 3- α -OH and His99, as depicted in Fig. 6M–P. For compounds with 3- α -OH sites, their 3-hydroxyl orientations precluded the formation of hydrogen bonds with His99 (Fig. 6M–O). For OCB, it seemed that the presence of an aldehyde group at C19 interacting with the 3-OH site, which result in a conformational rotation of the 3-OH site (Fig. 6P). The chemscore was used to estimate the binding affinity between the bufadienolides and SULT2A1. The chemscore values for the different bufadienolide substrates are listed in Table S3.[†] The chemscore values correlated with the experimental K_m results. For example, CBFT had the lowest chemscore value of -36.68 , and the lowest K_m for SULT2A1. BFE had the highest K_m and chemscore values. When comparing the experimental potency, we found that the binding affinities of GB, AB and BFT were correlated with the results obtained from the *in vitro* assays. However, there were several exceptions; for example, DBT had a low affinity for SULT2A1, but the chemscore value was -35.18 . The disagreement between the molecular modeling results and the *in vitro* results may be due to the complex interaction mechanisms between substrates and enzyme.

Discussion

Sulfate conjugation by cytosolic sulfotransferases is an important biotransformation reaction in the metabolism of drugs, hormones, neurotransmitters, and xenobiotic compounds.²³ In the present study, 3-*O*-sulfation was found to be the common metabolic pathway of the six representative bufadienolides of amphibian skin secretion in human liver. The catalytic enzyme was identified as SULT2A1. Additionally, the 3- β -OH site was identified as the corresponding sulfate conjugation site of bufadienolides. Considering that bufadienolides with a 3- α -OH were not effectively catalyzed by rhSULT2A1, it indicated that the SULT2A1-mediated sulfate conjugation of bufadienolides was a regio- and stereo-selective reaction. The complicated interaction mode between bufadienolides and SULT2A1 were

explained by molecular docking study. It suggested that appropriate orientations and the formation of hydrogen bonds to key amino acid residues of the catalyst active site (His99) played important roles in the reaction (Fig. 6). The bufadienolides that could not form hydrogen bonding with His99 due to the non-preferred orientations of the 3-OH site were not efficaciously catalyzed by SULT2A1 (Fig. 6M–P). The results indicated that enclosing the 3- β -OH or introducing the chemical modifications which could hinder the formation of hydrogen bonding with His99 may increase the metabolic stability of bufadienolides by reducing the sulfation. As reported previously, two substrate-binding orientations have been identified for DHEA, including the primary, catalytic, orientation and the second alternative orientation.²⁴ In comparison with the primary orientation, the second orientation penetrates further into the active site (Fig. S6[†]). Additionally, there is a 45° rotation of the DHEA out of the steroid plane with respect to the catalytic orientation. As shown in Fig. S7,[†] the binding modes of all the bufadienolides were different from the primary catalytic orientation of the DHEA according to the docking analysis. They located close to the DHEA molecule in the proposed alternative orientation. The discrepancy may derive from the difference in structures of bufadienolides and DHEA. Considering that the active site of SULT2A1 was hydrophobic in nature, the inclusion of α -pyranone of bufadienolides may give rise to more hydrophobic interaction which leading to the difference between the primary binding orientation of bufadienolides and DHEA.

The kinetic characterizations performed herein demonstrated that the 3-*O*-sulfation of bufadienolides with marked variations in the apparent K_m and intrinsic clearance values. In comparison, RB and BFT showed the highest and lowest intrinsic clearance values, respectively, and varied by hundreds-fold. This was attributed to the evident differences of their affinities and maximum rates in the conjugation reactions. The structure–sulfation relationship could be summarized as follows: SULT2A1 shows stereo-selectivity for the 3-OH sites of bufadienolides, but not the 3- α -OH sites. Hydrophilic group substitutions (such as hydroxyl substations at the C11, C14 and C16 positions) typically decrease the binding affinities, with an exception for hydroxyl substitutions at the C5 positions, which reversely increases the binding affinities (potentially attributed

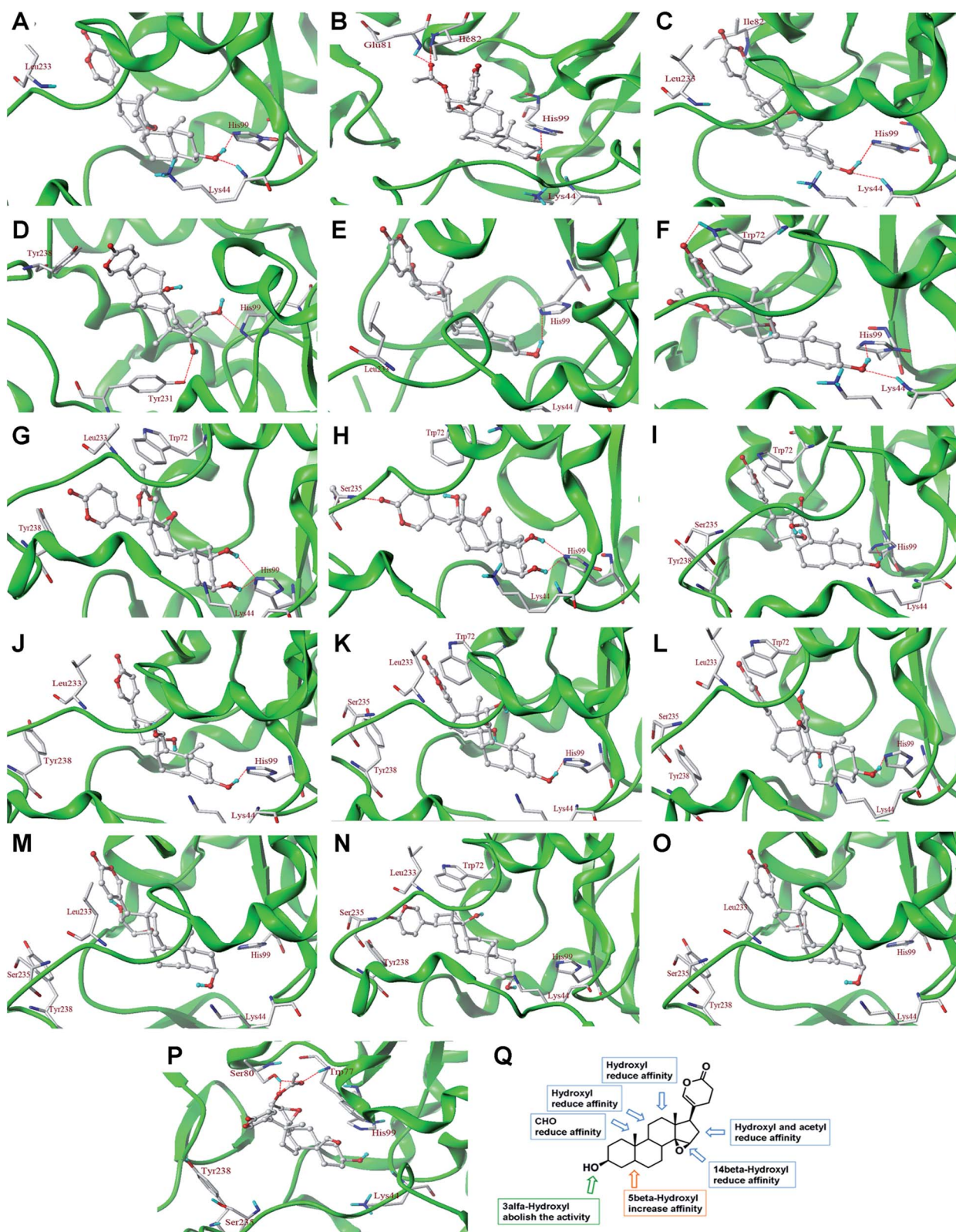


Fig. 6 The interaction binding modes and structural relationships of bufadienolide derivatives with SULT2A1. (A–P) The interaction binding mode of (A) RB; (B) CB; (C) BF; (D) TCB; (E) DCB; (F) BFT; (G) CBFT; (H) DABT; (I) AB; (J) GB; (K) PBFE; (L) BFE; (M) EDCB; (N) EBF; (O) ERB; (P) OCB with SULT2A1, where C, O, N and H atom were colored grey, red, blue and cyan, respectively. (Q) The relationships between chemical structures and affinity toward SULT2A1.

to the inclination to form additional hydrogen bonds that further enhance the interaction between the bufadienolides and active site, as shown in Fig. 6F). The aldehyde group at the C19 position prevents the sulfation processes. The OAc residue at C16 decreased the affinity for SULT2A1. It should be noted that the C5 position hydroxylation has been identified as the major phase I metabolic reaction in our previous studies.^{3,15,16} Thus, the increased binding affinities due to hydroxyl substitutions at C5 indicated a potent interplay between the phase I and phase II metabolic routes of bufadienolides. The above information could provide guidance for optimization the metabolic stability of bufadienolides.

Hitherto, the most commonly used probe substrate of SULT2A1 is endogenous steroid DHEA.^{19,25,26} However, it should be noted that DHEA is not highly selective catalyzed by SULT2A1 due to the participation of SULT1E1.²⁷ In the present study, SULT2A1 showed strong selectivity and specificity toward the sulfation of the six studied bufadienolides. Although SULT2A1 and SULT1E1 are common sulfotransferases in the sulfation of steroids,²⁰ it had been reported that a large steric group at the D-ring of steroids hindered the entrance of compounds into the binding pocket of SULT1E1.²⁸ Therefore, the high catalytic selectivity may attribute to the characteristic structural feature of α -pyrone attached at the C17 position. Additionally, from the perspectives of *enzyme activity quantification*, our results showed that DCB 3-O-sulfation displayed the weak substrate inhibition and relatively high catalysis rate. The high specific and appropriate kinetic behaviors all suggested that DCB could be a better probe for detection the activity of human SULT2A1.

In humans, SULT2A1 is responsible for catalyzing the sulfation of hydroxysteroids, including DHEA, androgens and pregnenolone, and bile acids.^{19,29} The SULT2A1-mediated sulfation of steroids has been reported to be an important process for maintaining steroid hormone (such as deoxycorticosterone and dehydroepiandrosterone) levels.³⁰ For example, the apparent K_m of the SULT2A1-mediated sulfation of RB was 0.45 μ M, which was almost 5-fold lower than that of DHEA, indicating the potential regulation of DHEA levels by bufadienolides. Additionally, the docking of non-substrate molecule did not result in a poor fitting score in our study (Table S3†). These results indicated that these compounds could also enter into the catalytic space of SULT2A1 and interact with the enzyme, but their orientations precluded the reaction. These all suggests that the bufadienolide constituents may increase the level of circulating unconjugated deoxycorticosterone and dehydroepiandrosterone by inhibiting their conjugation. The potential for endocrine disruption by this mechanism or alterations to the metabolism of drugs or other xenobiotics through the inhibition of SULT2A1 requires further evaluation.

It is important to understand the differences of metabolism, especially the prominent inactivated pathway in selecting the appropriate animal model and in the interpretation of data from studies with animals. However, the data presented herein and elsewhere suggest major inter-species differences in sulfation and SULT enzyme profiles.³¹ As a whole, the present qualitative and quantitative interspecies study of BF and RB sulfation showed that the monkey, mini-pig, rabbit and guinea

pig exhibited similar metabolic profiles, kinetic behaviors and intrinsic metabolic clearances of BF and RB sulfate conjugation with those of human. However, it found that the sulfate conjugates of the bufadienolides were undetectable when RB and BF were incubated with liver S9 from dog and mouse. The results reflected a weak and deficient capacity of the SULT2A1 in the livers of dogs and mice, which was further confirmed by using endogenous substrate DHEA (data not shown). Additionally, the variation on K_m values for BF and RB sulfation between HLS9 and RLS9 indicated the different catalytic behavior of human and rat SULT in response to bufadienolide. These results implied that mouse, rat and dog models are not suitable for simulating RB and BF sulfations in humans, and the *in vivo* data obtained from the aforementioned animals should be cautiously utilized.

Conclusions

The sulfation of bufadienolides was fully characterized in the present study. The conjugate metabolites of bioactive bufadienolides examined were identified as 3-O-sulfates in human primary hepatocyte, and SULT2A1 was the specific isoform responsible for the conjugation reaction with high regio- and stereo-selectivity. The interaction mode between bufadienolides and SULT2A1 was first elucidated by model docking studies. The results indicated the importance of appropriate orientations and hydrophobic interactions between the ligands and His99 residue of SULT2A1. Moreover, the bufadienolides-sulfation relationship was elucidated and sulfation of DCB is verified to be a highly selective probe reaction for human SULT2A1. Additionally, a significant species-dependent variation in sulfation pathway was also found. Our improved understanding of bufadienolides-SULT interaction will provide guidance for the rational use of bufadienolides in the clinic or insight into the bufadienolides-sulfation relationship in human.

Materials and methods

Materials

Bufalin (BF), resibufogenin (RB), cinobufagin (CB), bufotalin (BFT), telocinobufagin (TCB), deacetylcinobufagin (DCB), cinobufotalin (CBFT), gamabufotalin (GB), deacetylbufotalin (DBT) were purchased from Shanghai Boyle Chemical Company (Shanghai, China). Other bufadienolides were isolated from amphibian skin secretion or obtained by biotransformation using microorganisms by the author (J. Ning) and unambiguously identified by NMR and MS techniques. Their purities were greater than 98% as determined by high-performance liquid chromatography with diode-array detection (HPLC/DAD). A mixed pool of human liver S9 (HLS9), individual human liver S9, and pooled liver S9 of male ICR/CD-1 mice (MLS9), male Sprague-Dawley rats (RLS9), male Dunkin-Hartley guinea pigs (GLS9), male New Zealand rabbits (RaLS9), male Beagle dogs (DLS9), male Yucatan mini-pigs (PLS9) and male Cynomolgus monkeys (CyLS9) were purchased from Research Institute for Liver Diseases (RILD, Shanghai, China). Recombinant human

SULTs (rhSULT) were obtained from BD Gentest (Woburn, MA, USA). Mixed, pooled human hepatocytes were purchased from Celsis *In vitro* Technologies (Baltimore, MD, USA). Dehydroepiandrosterone (DHEA), 6-dichloro-*p*-nitrophenol (DCNP), dithiothreitol (DTT), estrone, ibuprofen, quercetin, 3'-phosphoadenosine-5'-phosphosulfate (PAPS) were purchased from Sigma-Aldrich (St. Louis, MO, USA). All other reagents were either of liquid chromatography (LC) grade or the highest grade commercially available.

Incubation system and analysis method

The standard incubation system for SULT reactions included HLS9 or rhSULTs, DTT (8 mM), PAPS (1 mM), potassium phosphate buffer (50 mM, pH 7.4), MgCl₂ (5 mM), and substrates in a final volume of 200 μ L. After pre-incubation at 37 °C for 3 minutes, the SULT reaction was initiated by adding PAPS and further incubated at 37 °C in a water bath under constant shaking. The reaction was terminated by the addition of ice-cold methanol (100 μ L). The mixture was kept on ice until pelleting at 20 000 g for 10 minutes at 4 °C. Aliquots of supernatants were stored at -20 °C until analyses. Control incubations without PAPS, substrate or S9 were performed to ensure that the metabolites produced were S9- and PAPS-dependent.

The Agilent 1200 HPLC system consisted of a quaternary delivery system, a degasser, an auto-sampler and a UV-detector. An Elite A SinoChrom ODS-BP (2.1 \times 150 mm, 5 μ m) analytical column was used for quantification. The mobile phase consisted of an acetonitrile-0.1% formic acid aqueous solution at a flow rate of 0.45 mL min⁻¹. An Applied Biosystems MDS Sciex Qtrap 4500 Triple Quadrupole Mass Spectrometer (MS/MS) equipped with an electrospray ionization (ESI) source was used to analyze the target metabolites. The system was operated in negative mode for BF-S (*m/z* 465.5–466.5), RB-S (*m/z* 462.5–463.5), CB-S (*m/z* 520.7–521.7), BTF-S (*m/z* 522.4–523.4), TCB-S (*m/z* 480.8–481.8), and DCB-S (*m/z* 478.7–479.7). The negative ion spray voltage and temperature were set at -4500 V and 600 °C, respectively. The curtain gas and collision-activated dissociation gas were set at 10 psi and 5 psi, respectively; gas1 and gas2 (nitrogen) were set at 30 L min⁻¹ and 45 L min⁻¹, respectively. The dwell times were 150 ms.

Synthesis of metabolites and NMR spectroscopy

The sulfated metabolites of BF, RB, CB, BFT, TCB and DCB were produced *in vitro*. Briefly, the six compounds were each added to the pyridine reaction mixture (2 mL), which contained sulfuric acid (11.9 mg, 0.12 mM) and acetic anhydride (0.12 mM). After each mixture was stirred for 60 minutes at 60 °C, the reaction was quenched with 2 mL aqueous NH₃ (25%). The resultant residue was isolated and purified by reverse-phase-column chromatography (methanol : H₂O = 1 : 2). The purities of the six bufadienolides sulfate metabolites were all above 98% as determined by HPLC-DAD analyses.

All NMR experiments were performed on a Varian INOVA-500 NMR spectrometer. ¹H and ¹³C NMR spectra (500 MHz) were measured at room temperature (22 °C). Chemical shifts are

shown in the δ scale and were referenced to tetramethylsilane at δ = 0 ppm for the ¹H and ¹³C spectra.

Recombinant SULT assay

The rhSULT (1A1*1, 1A1*2, 1A2, 1A3, 1B1, 1E1, and 2A1) were used to screen the involved isoform(s) in the sulfation of the six bufadienolides in HLS9. Three substrate concentrations (1, 10 and 100 μ M) were incubated with each of the rhSULT (0.02 to 0.2 mg mL⁻¹) at 37 °C for 60 minutes. The incubations with isoforms were carried out under standard assay procedures described in the text.

Kinetics characterization

To estimate the kinetics parameters, the six compounds were incubated with HLS9, rhSULT2A1 and complex recombinants, which consisted of different proportions of rhSULT1A1*1, 1A1*2, 1A2, 1B1, 1E1, and 2A1, respectively, according to their hepatic contents in humans.¹⁹ The incubation conditions were optimized to ensure that formation rates of metabolites were in the linear range in relation to incubation time and protein concentration. The assays with HLS9 were conducted with a different protein concentration of 0.2 mg mL⁻¹ (BF), 0.06 mg mL⁻¹ (RB), 0.4 mg mL⁻¹ (CB), 0.6 mg mL⁻¹ (BFT), 0.2 mg mL⁻¹ (TCB), and 0.2 mg mL⁻¹ (DCB) for 30–60 min, respectively. The assays with SULT2A1 were conducted with a different protein concentration of 0.02 mg mL⁻¹ (BF), 0.006 mg mL⁻¹ (RB), 0.02 mg mL⁻¹ (CB), 0.06 mg mL⁻¹ (BFT), 0.006 mg mL⁻¹ (TCB), and 0.02 mg mL⁻¹ (DCB) for 30–50 min, respectively. The assays with complex isoforms were conducted with a different protein concentration of 0.06 mg mL⁻¹ (BF), 0.02 mg mL⁻¹ (RB), 0.06 mg mL⁻¹ (CB), 0.2 mg mL⁻¹ (BFT), 0.04 mg mL⁻¹ (TCB), and 0.06 mg mL⁻¹ (DCB) for 30–60 min, respectively.

To further explore the interaction between the bufadienolide derivatives and SULT2A1, kinetics analyses of other bufadienolide derivatives with classical structural features (Fig. S2†) were also carried out by using rhSULT2A1. The incubation conditions were optimized as described.

Chemical inhibition study

The six compounds were incubated with HLS9 in the presence or absence of human SULT specific inhibitors or substrates, including the SULT1A1 specific inhibitor mefenamic acid (0.5 μ M),³² the SULT1E1 specific inhibitor ibuprofen (500 μ M), estrone (1 μ M),^{32,33} the SULT2A1 substrate DHEA (10 μ M) and general inhibitors DCNP (10 μ M) and quercetin (1 μ M) (which inhibit SULT1A1 and SULT1E1).³⁴ To further assess the role of SULT2A1, the inhibitory effects of DHEA (0–50 μ M) toward the sulfation of the six compounds catalyzed by HLS9 and SULT2A1 were investigated. The IC₅₀ values were also determined.

Correlation study

The formation rates of the sulfate metabolites of the six compounds were compared with the rate of DHEA sulfation using 16 individual HLS9 *via* linear regression analyses. The

concentration of DHEA was 4 μM (near its K_m). The six compounds were incubated in HLS9 at protein concentrations of 0.02 mg mL⁻¹ (BF), 0.12 mg mL⁻¹ (RB), 0.4 mg mL⁻¹ (CB), 0.8 mg mL⁻¹ (BFT), 0.6 mg mL⁻¹ (TCB) and 0.4 mg mL⁻¹ (DCB) for 30 minutes. Spearman's rank method was used to determine the correlation analysis of HLS9 from the 16 individual donors. When the r value was greater than or equal to 0.5 and the p value was less than 0.05, the correlations were considered significant.

Interspecies variation in the sulfate conjugation

RB and BF were selected to study the interspecies variation in the sulfation of bufadienolides due to their natural abundance and potent biological activities (toxicity), respectively. The kinetics characterizations were performed using liver S9 from different animal species, including monkey, mini-pig, dog, rabbit, guinea pig, rat and mouse. The incubation conditions were the same as previously mentioned. The protein concentration of the liver S9 obtained from monkey, pig, rabbit, guinea pig and rat were 0.4, 0.2, 0.04, 0.2 and 0.6 mg mL⁻¹ for BF study and 0.2, 0.06, 0.06, 0.06 and 0.2 mg mL⁻¹ for RB study, respectively.

Docking studies

The molecular docking studies were performed using the Surflex-Dock of the SYBYL procedure to explore potential binding modes between bufadienolides and the SULT2A1 protein complex. Surflex-Dock used an empirical scoring function and a patented search engine to dock ligands into a protein's binding site. The crystal structure of SULT2A1 with ligand DHEA (PDB: 1J99) was used as a receptor. The active pocket for substrate binding was generated around the crystallographic ligand in an automatic mode with the float radius at zero. Bufadienolides were docked into the active site of SULT2A1 to provide insights into the interaction modes. Each ligand was generated for 20 conformations.

Data analysis and statistics

The kinetics constants for bufadienolides sulfation by HLS9 or rhSULT2A1 were obtained by fitting the experimental data to Corporation, Northampton, MA). The substrate inhibition the substrate inhibition kinetics using Origin (OriginLab equation is $V = V_{\text{max}} \times [S]/(K_m + [S] + [S]^2/K_{\text{si}})$, where V is the velocity of reaction, V_m is the maximal velocity, K_m is the substrate concentration at half the maximal velocity, K_{si} is the constant describing the substrate inhibition interaction, and $[S]$ is the substrate concentration. The IC_{50} represents the inhibitor concentration that inhibits 50% of control activity and is determined by nonlinear curve fitting with Origin. All incubations were performed in three independent experiments in duplicate. Kinetic constants and IC_{50} values are reported as the value \pm S.E. of the parameter estimate.

Acknowledgements

We thank the National Natural Science Foundation of China (81473334, 81274047, 81503201, and 81503152), Distinguished

Professor of Liaoning Province, Dalian Outstanding Youth Science and Technology Talent (2014J11JH132, 2015J12JH201), Project sponsored by Liaoning BaiQianWan Talents Program and Innovation Team of Dalian Medical University for financial support.

References

- 1 J. B. Puschett, E. Agunanne and M. N. Uddin, *Am. J. Kidney Dis.*, 2010, **56**, 359–370.
- 2 H. Gao, R. Popescu, B. Kopp and Z. Wang, *Nat. Prod. Rep.*, 2011, **28**, 953–969.
- 3 X. C. Ma, J. Ning, G. B. Ge, S. C. Liang, X. L. Wang, B. J. Zhang, S. S. Huang, J. K. Li and L. Yang, *Drug Metab. Dispos.*, 2011, **39**, 675–682.
- 4 T. Mijatovic, F. Dufrasne and R. Kiss, *Curr. Med. Chem.*, 2012, **19**, 627–646.
- 5 Z. Meng, P. Yang, Y. Shen, W. Bei, Y. Zhang, Y. Ge, R. A. Newman, L. Cohen, L. Liu, B. Thornton, D. Z. Chang, Z. Liao and R. Kurzrock, *Cancer*, 2009, **115**, 5309–5318.
- 6 D. L. Wang, F. H. Qi, H. L. Xu, Y. Inagaki, Y. Orihara, K. Sekimizu, N. Kokudo, F. S. Wang and W. Tang, *Mol. Med. Rep.*, 2010, **3**, 717–722.
- 7 H. Zhao, X. Wu, H. Wang, B. Gao, J. Yang, N. Si and B. Bian, *J. Sep. Sci.*, 2013, **36**, 492–502.
- 8 R. A. Newman, P. Yang, A. D. Pawlus and K. I. Block, *Mol. Interventions*, 2008, **8**, 36–49.
- 9 T. Mijatovic and R. Kiss, *Planta Med.*, 2013, **79**, 189–198.
- 10 J. A. Salvador, J. F. Carvalho, M. A. Neves, S. M. Silvestre, A. J. Leitão, M. M. Silva and M. L. Sá e Melo, *Nat. Prod. Rep.*, 2013, **30**, 324–374.
- 11 S. Toma, S. Morishita, K. Kuronuma, Y. Mishima, Y. Hirai and M. Kawakami, *Xenobiotica*, 1987, **17**, 1195–1202.
- 12 Y. Shimizu and S. Morishita, *Am. J. Chin. Med.*, 1996, **24**, 289–303.
- 13 Y. Cao, L. Zhao, Q. Liang, K. Bi, Y. Wang and G. Luo, *J. Chromatogr. B: Anal. Technol. Biomed. Life Sci.*, 2007, **853**, 227–233.
- 14 F. Li, Y. Weng, L. Wang, H. He, J. Yang and X. Tang, *Int. J. Pharm.*, 2010, **393**, 203–211.
- 15 G. B. Ge, J. Ning, L. H. Hu, Z. R. Dai, J. Hou, Y. F. Cao, Z. W. Yu, C. Z. Ai, J. K. Gu, X. C. Ma and L. Yang, *Chem. Commun.*, 2013, **49**, 9779–9781.
- 16 J. Ning, Z. L. Yu, L. H. Hu, C. Wang, X. K. Huo, S. Deng, J. Hou, J. J. Wu, G. B. Ge, X. C. Ma and L. Yang, *Drug Metab. Dispos.*, 2015, **43**, 299–308.
- 17 K. Shimada, K. Ohishi, H. Fukunaga, J. S. Ro and T. Nambara, *J. Pharmacobio-Dyn.*, 1985, **8**, 1054–1059.
- 18 O. A. Akimova, A. Y. Bagrov, O. D. Lopina, A. V. Kamernitsky, J. Tremblay, P. Hamet and S. N. Orlov, *J. Biol. Chem.*, 2005, **280**, 832–839.
- 19 Z. Riches, E. L. Stanley, J. C. Bloomer and M. W. Coughtrie, *Drug Metab. Dispos.*, 2009, **37**, 2255–2261.
- 20 Z. E. Tibbs, K. J. Rohn-Glowacki, F. Crittenden, A. L. Guidry and C. N. Falany, *Drug Metab. Pharmacokinet.*, 2015, **30**, 3–20.
- 21 I. T. Cook, T. S. Leyh, S. A. Kadlubar and C. N. Falany, *Horm. Mol. Biol. Clin. Invest.*, 2010, **1**, 81–87.

- 22 O. Pelkonen, M. Turpeinen, J. Uusitalo, A. Rautio and H. Raunio, *Basic Clin. Pharmacol. Toxicol.*, 2005, **96**, 167–175.
- 23 N. Gamage, A. Barnett, N. Hempel, R. G. Duggleby, K. F. Windmill, J. L. Martin and M. E. McManus, *Toxicol. Sci.*, 2006, **90**, 5–22.
- 24 P. H. Rehse, M. Zhou and S. X. Lin, *Biochem. J.*, 2002, **364**, 165–171.
- 25 B. A. Thomae, B. W. Eckloff, R. R. Freimuth, E. D. Wieben and R. M. Weinshilboum, *Pharmacogenomics J.*, 2002, **2**, 48–56.
- 26 E. B. Yalcin, V. More, K. L. Neira, Z. J. Lu, N. J. Cherrington, A. L. Slitt and R. S. King, *Drug Metab. Dispos.*, 2013, **41**, 1642–1650.
- 27 M. Suiko, Y. Sakakibara and M. C. Liu, *Biochem. Biophys. Res. Commun.*, 2000, **267**, 80–84.
- 28 E. V. Petrotchenko, M. E. Doerflein, Y. Kakuta, L. C. Pedersen and M. Negishi, *J. Biol. Chem.*, 1999, **274**, 30019–30022.
- 29 K. A. Comer, J. L. Falany and C. N. Falany, *Biochem. J.*, 1993, **289**, 233–240.
- 30 H. J. Chang, R. Shi, P. Rehse and S. X. Lin, *J. Biol. Chem.*, 2004, **279**, 2689–2696.
- 31 M. W. Coughtrie, *Pharmacogenomics J.*, 2002, **2**, 297–308.
- 32 R. S. King, A. A. Ghosh and J. Wu, *Curr. Drug Metab.*, 2006, **7**, 745–753.
- 33 L. Wang, N. Raghavan, K. He, J. M. Luetgen, W. G. Humphreys, R. M. Knabb, D. J. Pinto and D. Zhang, *Drug Metab. Dispos.*, 2009, **37**, 802–808.
- 34 T. Walle, E. A. Eaton and U. K. Walle, *Biochem. Pharmacol.*, 1995, **50**, 731–734.